ARI The Bulletin of the Istanbul Technical University VOLUME 53, NUMBER 1
Communicated by Derin Orhon

Determining the Non-Linear Behavior of 3D, R-C Shear Wall-Frame Structures with a Stochastic Approach

Beyza Taşkın and Zeki Hasgür
Department of Civil Engineering, Istanbul Technical University, 34469 Maslak, Istanbul, Turkey
(Received 16 April 2003)

Stochastic analysis of reinforced concrete (R-C) 3D shear wall-frame structures under seismic excitations with the emphasis on the analysis of stiffness and strength degradation due to plastic deformations is theoretically performed. As constitutive moment-curvature relation, the model of extended Roufaiel-Meyer for flexural behavior and for shear reversals Origin-Oriented hysteretic model have been examined by making some modifications for wall elements and frame members. Stochastic earthquake excitations are specified as intensity modulated to the Jennings-Housner-Tsai type envelope function and Gaussian white noise filtered simulated earthquake. Dynamic equation of motion is formed as an equivalent first order Stratonovich stochastic differential equation. In order to reduce the calculation time during extensive simulations, a system reduction scheme have been implemented. Demonstrating the ability of the program to predict the actual seismic response, a 7 storey R-C wall-framed full-scale test structure has been calculated and the results are successfully compared with the experimentally recorded data.

Keywords: Non-linear analysis, wall-frame structures, white noise, stochastic.

1. Introduction

While analyzing the seismic response of R-C elements, material non-linearity should be handled as well as unsymmetrical cross-sections with different yield capacities at positive and negative bending, stiffness and strength degradation during plastic deformations and finite extensions of plastic zones at the end of the structural elements. Depending on different characteristics of the R-C members consisting the structural system during seismic loading, they are examined separately. For the mentioned analysis including the above considerations, the following essential assumptions are made.

i. All deformations of beams and columns are small compared to their lengths.

ii. Bernoulli's hypothesis is accepted.

iii. Influence of shear deformations is ignored for beams and columns.

iv. Increments of axial forces and torsional moments depend linearly on the increments of the axial elongation and the angular displacement, respectively.

v. Incremental constitutive moment-curvature relation with respect to local bending axes of an element is assumed to be decoupled.

vi. Inertial and linear viscous loadings are applied as external statically equivalent nodal loads.

2. Analysis of the Members of a Structural System

2.1. Beam and Column Elements

A beam/column element in the dynamically deformed state can be seen in Figure 1 utilizing the statical equilibrium as the reference. Here, the superscript $^{(0)}$ presents the stiff-body displaced state, while $^{(s)}$ denotes the statical equilibrium state before the excitation.

The displacement of the nodes and nodal loadings then can be written in the form,

$$\{r_e\}^T = \{r_3 \quad r_5 \quad r_9 \quad r_{11} \quad r_2 \quad r_6 \quad r_8 \quad r_{12} \quad r_4 \quad r_{10} \quad r_1 \quad r_7\} \tag{1}$$

$$\{R_e\}^T = \{V_{1z} \quad M_{1y} \quad V_{2z} \quad -M_{2y} \quad V_{1y} \quad -M_{1z} \quad V_{2y} \quad M_{2z} \quad M_{1x} \quad M_{2x} \quad N_1 \quad N_2\}. \tag{2}$$

Since the components of $\mathbf{R}_e$ are linearly dependent through the external equilibrium equations

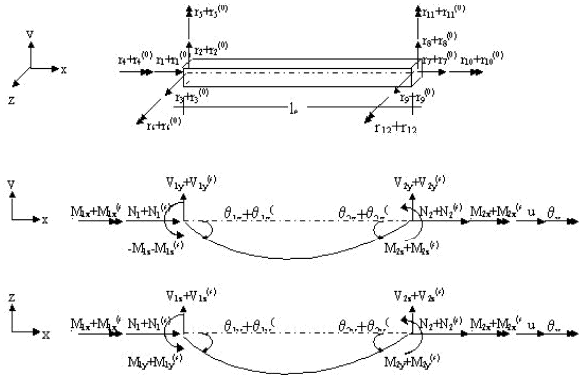

Figure 1. Nodal displacements and end forces of a 3D beam or column element.

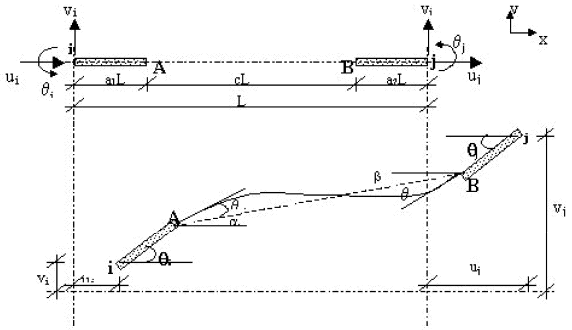

Figure 2. Nodal displacements of tie-beams with rigid supports at both nodes.

of the element, generalized stresses $\mathbf{Q}_e$ can be described by using six of these components.

$$\{Q_e\}^T = \left\{ \begin{array}{cccc} \tilde{M}_e^y & \tilde{M}_e^z & M_e^x & N \end{array} \right\},$$

$$\{M_e^y\} = \left\{ \begin{array}{c} M_{1y} \\ M_{2y} \end{array} \right\}, \quad \{M_e^z\} = \left\{ \begin{array}{c} M_{1z} \\ M_{2z} \end{array} \right\}. \qquad (3)$$

Here, it is obvious that N=N_1=N_2 and M_e^x=M_{1x}=M_{2x}. The nodal point displacements conjugated to $\mathbf{Q}_e$ can be written as,

$$\{q_e\}^T = \left\{ \begin{array}{cccc} \tilde{\theta}_e^y & \tilde{\theta}_e^z & \theta_e^x & u \end{array} \right\},$$

$$\{\theta_e^y\} = \left\{ \begin{array}{c} \theta_{1y} \\ \theta_{2y} \end{array} \right\}, \quad \{\theta_e^z\} = \left\{ \begin{array}{c} \theta_{1z} \\ \theta_{2z} \end{array} \right\}. \qquad (4)$$

By using the compatibility relations, the following equation can be written where **a** is the compatibility matrix [1].

$$\{\dot{q}_e\} = [a_e] \cdot \{\dot{r}_e\}. \qquad (5)$$

Using virtual work principle, the incremental stiffness relation can be written as,

$$\left\{\dot{Q}_e(t)\right\} = [k_e(t)] \cdot \{\dot{q}_e(t)\}, \qquad (6)$$

where $\mathbf{k}_e$(t) is the incremental stiffness matrix of the element.

2.2. Tie-Beam Elements

Although similar nodal displacements and loadings are present in tie-beams, the compatibility relations are different than beams and columns because of the rigid support at one or each end. Figure 2 illustrates the dynamically deformed tie-beam. Using the equilibrium equations, the following compatibility relation is obtained where $\mathbf{B}_c$ and $\mathbf{k}_{b,e}$ are the compatibility and stiffness matrices for tie-beams [2].

$$[k_{b,e}] = [B_c]^T [k_{el}] \cdot [B_c]. \qquad (7)$$

2.3. Wall Elements

Wall elements are determined consisting of n number of linear elastic segments having the same length similar as the study of [3]. Differently, all sub-elements have 12 DOF as seen in Figure 3. The value of n varies from 4 at higher storeys to 10 for the lower storeys. It is assumed that the moment distribution within the storey is linear and the corresponding curvature is constant for each wall segment. Since the bending or shear stiffness value may differ for each segment during non-linear effects, the stiffness matrices for each wall segment including the effect of shear deformations, should be obtained by [4]. Finally, condensed stiffness matrix $\mathbf{S}_e$ for the shear wall having 6 DOF at each storey levels (i) and $(i+1)$ is formed.

3. Hysteretic Models for Bending and Shear

In this study, an extended version of Roufaiel-Meyer hysteresis for defining the increments in bending properties for all type of elements and Origin-Oriented hysteretic model for shear reversals are used. Figures 4 and 5 show these relations, respectively.

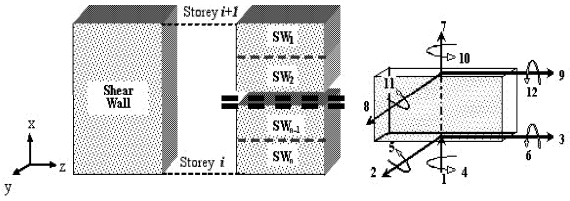

Figure 3. Division of wall element into segments.

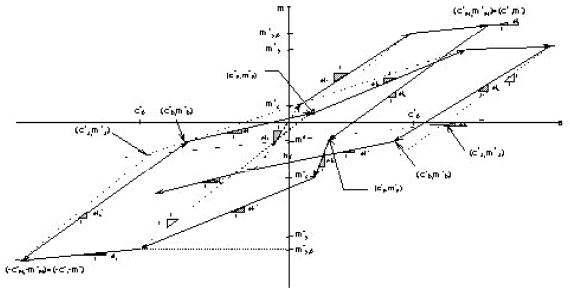

Figure 4. Roufaiel-Meyer hysteretic model for bending.

In the dimensionless relationship in Figure 4, $m_i(x)$ is the normalized value at the i.th branch of bending moment $M_i(x,t)$ with respect to yielding moment $M_y^+(x)$ and $c_i(x)$ is the corresponding normalized curvature.

In the model having six different loading and unloading branches both for positive and negative bending, the origin is settled at the normalized static moment $m^{(s)}(x)$ which is assumed to be less than the yield moment of the section with a bending stiffness of $ei_0=EI_{uc}/EI_{eq}$ where EI_{uc} is the bending stiffness of the uncracked section and EI_{eq} is the equivalent stiffness calculated by

$$EI_{eq}(x) = M_y^+(x)/\kappa_y^+(x). \tag{8}$$

The normalized bending stiffness value during the loading at a time t is calculated by

$$\begin{aligned} ei(x,t) \;=\; & ei_0(x,t)[\alpha_0^+(x,t) + \alpha_0^-(x,t)] + \\ & ei_1^+(x,t)\alpha_1^+(x,t) + ei_1^-(x,t)\alpha_1^-(x,t) + \\ & ei_2(x,t)\alpha_2(x,t) \;\; + ei_3^+(x,t)\alpha_3^+(x,t) + \\ & ei_3^-(x,t)\alpha_3^-(x,t) + ei_4^+(x,t)\alpha_4^+(x,t) + \\ & ei_4^-(x,t)\alpha_4^-(x,t) + ei_5^+(x,t)\alpha_5^+(x,t) + \\ & ei_5^-(x,t)\alpha_5^-(x,t), \end{aligned} \tag{9}$$

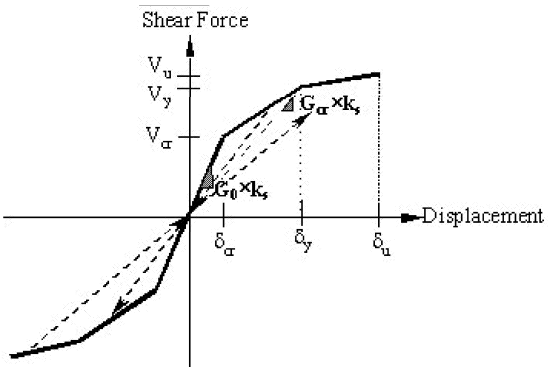

Figure 5. Origin-Oriented hysteretic model

where $\alpha_i^{\pm}$ are indicator functions with a value of 1 on the relevant loading branch and the value of 0 elsewhere. The points (c_p^+, m_p^+) and (c_p^-, m_p^-) where pinching occurs are controlled by α_p pinching factors as in [5]. For the strength degradation, the model introduced by [6] is used. According to this model, the strength reduction is controlled by utilizing the accumulated hysteretic energy, e(x,t), and commences when the ductility ratios c^+ or c^- exceed a critical normalized spalling curvature of c_s^+ or c_s^-, respectively. Then the strength reduction function, g(e), and the bending moment values can be written as

$$g(e) = \begin{cases} 1 & e \le e_0 \\ \exp\left(-\frac{e-e_0}{e_1}\right) & e > e_0, \end{cases}$$

$$m_y^{\pm}(x,t) = m_{y,0}^{\pm}(x) \cdot g\left[e\left(x,t\right)\right]. \tag{10}$$

where e_0 and e_1 are the parameters of the strength reduction function.

Figure 5 shows the shear force-displacement relation where V_{cr}, V_y and V_u are the cracking, yielding and ultimate shear forces within the element, respectively and δ_{cr}, δ_y and δ_u are the corresponding displacement values. G_0 is the shear modulus at the beginning and G_{cr} is the ratio of shear stress to strain at shear yielding. Presenting ρ as the ratio of transverse reinforcement, n the ratio of elasticity modulus of steel to concrete, A_{sh} as the effective area of wall, h the storey heigth, v shear stress in the wall and γ as the shear strain, the following equations can be written.

$$G_{cr} = \rho.n.G_0, \qquad V = v.A_{sh}$$

$$\delta_s = \gamma.h, \qquad v_y = \rho.f_{yk}. \tag{11}$$

Therefore the value of shear stiffness, K, varying on loading or unloading branches in the hysteretic model can be calculated according to the incremental G value as,

$$K = G \cdot \frac{A_{sh}}{h} = G \cdot k_s. \tag{12}$$

4. Modeling of Earthquake Motion

The acceleration process at the ground surface is determined as the response process of intensity modulated *Gaussian White Noise*, filtered through a Kanai-Tajimi filter with parameters ω_0 and ζ_0. The displacement of the earth surface r_0 relative to the bedrock surface is then related to the bedrock acceleration process $\{\ddot{r}_b(t), t \in [0, \infty)\}$is modeled as

$$\ddot{r}_0 + 2\zeta_0\omega_0\dot{r}_0 + \omega_0^2 r_0 = -\ddot{r}_b \tag{13}$$

Here, bedrock acceleration can be obtained from $\ddot{r}_b dt = \beta(t) \cdot dW(t)$ relation, where W(t) is a unit Wiener process and β(t) is a deterministic envelope function defined as (Jennings et al., 1968). The acceleration at the ground surface $\ddot{r}_s(t)$ is then be written as,

$$\ddot{r}_s(t) = (\ddot{r}_b + \ddot{r}_0) = (-2\zeta_0\omega_0\dot{r}_0 - \omega_0^2 r_0). \tag{14}$$

5. Dynamic System Analysis

The equation of motion in global coordinates is widely known as,

$$[M] \cdot \left\{\ddot{r} + \tilde{U}\ddot{r}_s\right\} + [C] \cdot \{\dot{r}\} + [K_{el} + G_* + S] \cdot \{r\}$$

$$+ [a_{pl}]^T \cdot \{Q_{pl}\} = 0. \tag{15}$$

r representing the vector of all transitional and rotational DOF, **M** and **C** mass and linear viscous damping matrices. In the expression, the subscripts $_{(el)}$ and $_{(pl)}$ define the members in elastic or plastic manner.

Using the compatibility and constitutive relations, the following equations are written,

$$\left\{\dot{Q}_{el}\right\} = [k_{el}] \cdot \{\dot{q}_{el}\},$$

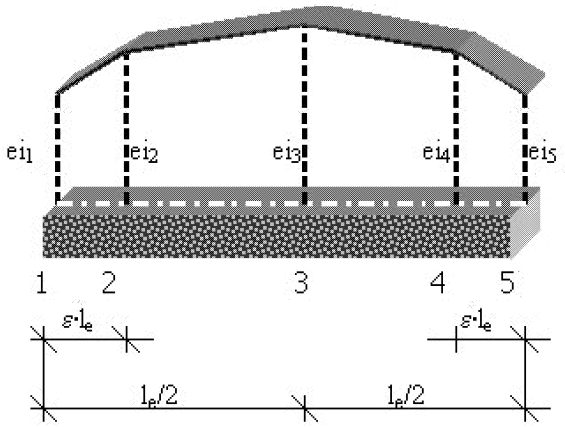

Figure 6. Variation of non-dimensional bending stiffness thru element length.

$$\left\{\dot{Q}_{pl}\right\} = \left[k_{pl}(\tilde{Q}_{pl}, \tilde{\dot{q}}_{pl}, \tilde{p}_{pl})\right] \cdot \{\dot{q}_{pl}\}, \tag{16}$$

where p_{pl} is the additional state variables from plastic elements.

During the calculation of the stiffness matrices, the normalized bending stiffness values $ci^{y,z}$ are determined by linear interpolation on five discrete points through the element length, l_e, for ξ_1=0, $\xi_2 = \varepsilon$, ξ_3=0.5, ξ_4=1-ε and ξ_5=1. Figure 6, illustrates these coordinates on a beam element where ε controls the length of plastic hinge.

Therefore, the dynamic equation of motion can be written in the following form.

$$\{\dot{q}\}^T \{Q\} = -\{\dot{r}\}^T [M] \{\ddot{r} + \{U\} \{\ddot{r}_0 + \ddot{r}_b\}\} \Rightarrow$$

$$[M]\{\ddot{r}\} + [a]^T \{Q\} = [M]\{U\}(2\zeta_0\omega_0\dot{r}_0 + \omega_0^2 r_0). \tag{17}$$

Then the dynamic equation of motion, filter equation and constitutive equations for R-C sections can be combined and written as an equivalent first order Stratonovich stochastic differential equation of the form,

$$d\{X(t)\} = \{F\{X\}\}dt + [\mathrm{G(t)}] \cdot d\{\mathrm{W}(t)\}, \tag{18.a}$$

$$\{F\{X\}\} = [A\{X\}].\{X\} + [K(\{Q_{pl}\}, [a_{pl}].\{\dot{r}\},$$

$$\{p_{pl}\})] \cdot [a_{pl}] \cdot \{\dot{r}\}, \tag{18.b}$$

$$\{X\}^T = \{\ \{r\} \quad \{\dot{r}\} \quad r_0 \quad \dot{r}_0 \quad \{Q_{pl}\} \quad \{p_{pl}\}\ \}^T,$$

$$[G(t)] = \left[\begin{array}{cccccc} \tilde{0} & \tilde{0} & 0 & -\beta(t) & \tilde{0} & \tilde{0} \end{array} \right]^T . \qquad (18.c)$$

where $\mathbf{X}$ is the state vector, $\mathbf{F}(\mathbf{X})$ is the drift vector, and $\mathbf{G}(\mathrm{t})$ is the diffusion matrix. The drift vector $\mathbf{F}(\mathbf{X},\mathrm{t})$ does only depend on explicitly on time if the filter coefficients are time-dependent. The diffusion vector $\mathbf{G}(\mathrm{t})$ is independent of the state vector $\mathbf{X}(\mathrm{t})$. Finally first order Stratonovich differential equation is solved using the 4^{th} order Runge-Kutta procedure for the response statistics of the system.

5.1. System Reduction

Since the time needed for calculations with the developed software depends on the dimension of the state vector $\mathbf{X}(\mathrm{t})$ which is dependent of the dimension N of the global displacement vector $\mathbf{r}$ and the plastic degree-of-freedom $\mathbf{q}_{pl}$, a system reduction scheme based on the truncated expansion of the eigenmodes of the undamaged structure is implemented as [7].

$$\{r(t)\} \cong \{\Phi\}^1 \cdot y_1(t) + \{\Phi\}^2 \cdot y_2(t) + ...$$

$$+\{\Phi\}^n \cdot y_n(t) = [\Phi] \cdot \{\mathrm{y(t)}\} \quad n \leq N. (19)$$

It should be noticed that, by applying n≤N to global displacement vector, elastic degrees of freedom are eliminated and the plastic degrees of freedom are maintained. Eigenmodes and the corresponding eigenfrequencies are obtained from the eigenvalue problem with Jacobi iteration.

$$[K_{el} + G_* + S] \cdot \{\Phi\}^i = \omega_{i,0}^2 \cdot [M] \cdot \{\Phi\}^i,$$

$$i = 1, 2, .., n. \qquad (20)$$

Therefore, the modal coordinates for the first n modes containing the non-linear behavior and for the rest with elastic behavior can be written as

$$\{y_{\mathrm{I}}\}^T = \left[\begin{array}{cccc} y_1 & . & . & y_n \end{array} \right],$$

$$\{y_{\mathrm{II}}\}^T = \left[\begin{array}{ccc} y_{n+1} & . & y_N \end{array} \right], \{y\} = \left\{ \begin{array}{c} \{y_{\mathrm{I}}\} \\ \{y_{\mathrm{II}}\} \end{array} \right\}, \quad (21)$$

and the corresponding orthonormalized modes will be

$$\left\{\bar{\Phi}\right\} = \left\{ \begin{array}{cc} \left\{\bar{\Phi}_{\mathrm{I}}\right\} & \left\{\bar{\Phi}_{\mathrm{II}}\right\} \end{array} \right\}. \qquad (22)$$

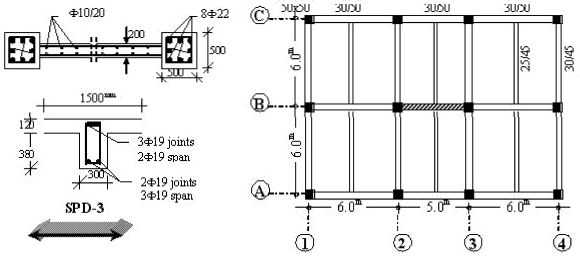

Figure 7. Full-scale, 7 storey BRI test structure

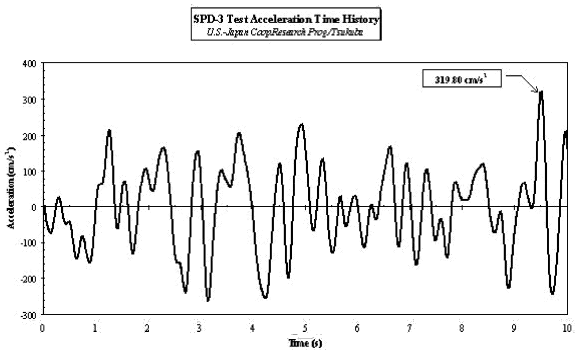

Figure 8. Modulated E-W component of 1952 Taft earthquake

When the same procedure is applied to the corresponding constitutive relations and if the quasi-static modal coordinates are ignored in the dynamic system equation, then equation of motion will only consist of the modal coordinates with non-linear behavior.

6. Numerical Example

In order to demonstrate the ability of the developed computer program SAR-CWF, a full-scale structure which is a part of the US-Japan Co-operative Research Program, constructed in Tsukuba-BRI is studied for comparison [8]. Figure 7 shows the floor plan and reinforcement details of the building.

All columns and walls are symmetrically reinforced, and further it is reported that the unit weight of concrete is γ_c=25 kN/m^3, the modulus of elasticity is E$_c$=2.5×10^7 kN/m^2, concrete compression strength f$_{ck}$=26.5 MPa, yield-

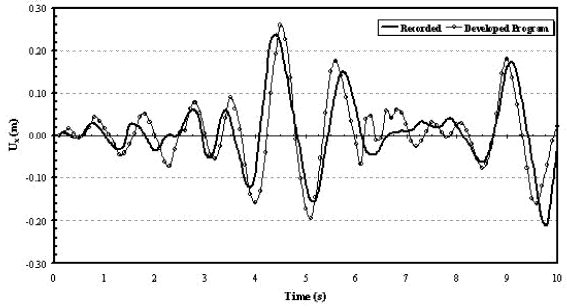

Figure 9. Top storey displacement time history of the 7 storey BRI test structure

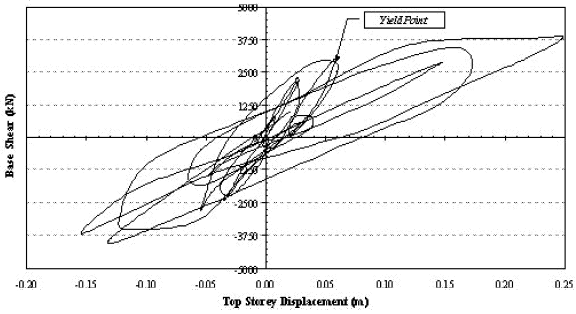

Figure 11. Top storey displacement - base shear variation

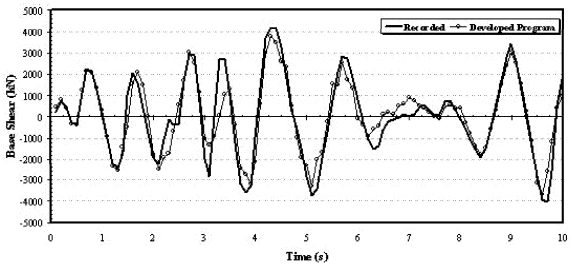

Figure 10. Base shear time history of the 7 storey BRI test structure

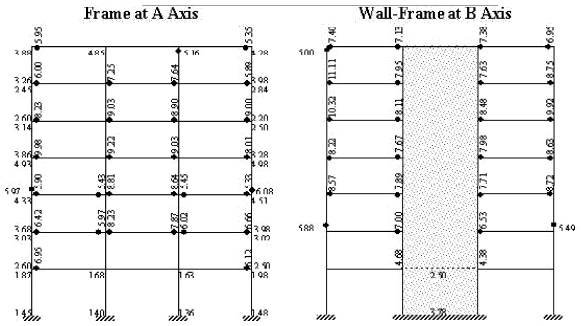

Figure 12. Plastic hinges and curvature ductilities

ing strength of steel is f_y=343 MPa, the Poisson's ratio υ=0.20 and the damping ratio for the structure is ξ=0.005. Detailed characteristic values for the elements' cross-sections such as moment of inertia for local axes, effective area, yield capacity for both positive and negative bending, cracking, yielding and ultimate shear capacities and the corresponding deformations for walls are used as in [9].

The pseudo-dynamically tested 7 storey shear wall-frame structure was subjected to modulated 1952 Taft Earthquake of E-W component (SPD-3) given in Figure 8.

For the analysis, shear walls at top five storeys are divided into 5 sub-elements, while 10 subdivisions are realized for the first and second storeys, since those correspond the critical height according to the Turkish Earthquake Resistant Design Code (1997). For the non-linear analysis, a time step of Δt=0.005 sec, strain hardening ratio of s(x)=0.10, distance controller for the plastic hinge length ε=0.10 and the parameters for the strength deterioration model e_0=26 and e_1=12 are used. From the eigen solutions of the linear system, the first two eigen periods are found out to be $T_{0,1}$=0.46 s and $T_{0,2}$=0.12 s, respectively.

After SPD-3 strong motion with a peak acceleration of $\approx$320 cm/s^2 is applied to the system, the first two periods of the system increased to T_1=0.87 s and T_2=0.18 s, respectively which are very close to the values reported during the experiments [10]. The top storey displacement variation and base shear time history are also investigated. The comparison of the calculated values and the recorded data for these terms can be seen in Figures 9 and 10, respectively.

For evaluating the displacement ductility of the structure, top storey displacement versus base shear relation is obtained similar to [11]. According to Figure 11, the ductility is calculated

as 4.32, which is reported as 4.10 after the tests. Furthermore, the occurrence of plastic hinges and the values of curvature ductilities calculated by the program are very close to the ones recorded during the tests [12]. Figure 12 shows a scheme for hinges and the curvature ductility values.

7. Conclusions

A computer program for the non-linear stochastic analysis of 3D RC shear wall-frame structures is developed including the properties of unsymmetrical cross-sections with different yield capacities, interaction of bending moments and axial forces, stiffness and strength degradation due to plastic deformations, pinching effect of moment-curvature relation and finite extensions of plastic hinges. Application of an extended version of Roufaiel-Meyer hysteretic model for bending and Origin-Oriented hysteretic model for shear reversals is carried out. A system reduction scheme based on a truncated expansion of the eigenmodes of the undamaged structure has been realized. Finally, by gathering the dynamic equation of motion, filter equation and constitutive relations together, first order Stratonovich stochastic differential equation for the system is obtained.

The capabilities of the program have been demonstrated by a numerical example which is a full-scale test structure. Depending on the comparison of the deterministic analysis results and the test records, it can be concluded that prediction of the magnitudes of peak values and their frequencies for both top storey displacement and base shear time histories as well as the displacement and curvature ductility values and the formation of plastic hinges are found to be successful.

It is aimed to run the software for many realizations of strong motion ensemble and obtain the response statistics of structural elements. Besides ensemble averages like expected values, standard deviations or higher order statistics of the element responses, suitable probability distribution functions are also required and have to be researched for probabilistic and reliable design of structures subjected to earthquake loading.

References

[1] K. J. Mørk, Stochastic Response Analysis of 3D Reinforced Concrete Structures Under Seismic Excitation, Structural Reliability Theory, 99, Un. Aalborg, Denmark. (1992).

[2] B. Taşkın, Ph.D. Thesis, Istanbul Technical University, Istanbul, Turkey (2001).

[3] R. R. Lopez, Ph.D. Thesis, University of llinois, Urbana Champaign, U.S.A. (1988).

[4] J. S. Przemienniecki, Theory of Matrix Structural Analysis, (McGraw-Hill Book Company, New York 1968).

[5] M. S. L. Roufaiel and C. Meyer, Journal of Structural Engineering, ASCE, **113**, 429 (1987).

[6] N. B. Kristensen and K. Nørgaard, M.Sc.Thesis, University of Aalborg, Denmark. (1992).

[7] K. J. Mørk and S. R. K. Nielsen, System Reduction for Random Dynamically Loaded Elasto-Plastic Structures, Proceedings of the Scandinavian Forum on Stochastic Mechanics, Sweeden, 145 (1991).

[8] T. Kabeyasava, H. Shiohara, S. Otani, and H. Aoyama, Journal of Faculty of Engrg., University of Tokio, **XXXVII**, 431 (1983).

[9] M. Midorikawa and Y. Kitagawa, U.S.-Japan Cooperative Research on R/C Full-Scale Building Test, Part 4: Dynamic Characteristics of the Building, Proceedings of the 8^{th} World Conf. on EQ Eng., VI, USA, July 21-28, 619 (1984).

[10] Turkish Earthquake Resistant Design Code. Ministry of Public Works and Settlement, Ankara (1997).

[11] T. Kabeyasava, H. Shiohara, S. Otani, and H. Aoyama, U.S.-Japan Cooperative Research on R/C Full-Scale Building Test, Part 5: Discussion of Dynamic Response of the System. Proceedings of the 8^{th} World Conf. on EQ Eng., VI, USA, July 21-28, 627 (1984).

[12] S. Okamoto, Y. Kitagawa, S. Nakata, M. Yoshimura, and T. Kaminosono, U.S.-Japan Cooperative Research on R/C Full-Scale Building Test, Part 2: Damage Aspects and Response Properties Before Repair Works. Proceedings of the 8^{th} World Conf. on EQ Eng., VI, USA, July 21-28, 603-610. (1984).

[13] M. Yoshimura and H. Tsubosaki, U.S.-Japan Cooperative Research on R/C Full-Scale Building Test, Part 6: Ultimate Moment-Resisting Capacity, Proceedings of the 8^{th} World Conf. on EQ Eng., VI, USA, July 21-28, 635-642 (1984).